J|A|C|S
ARTICLES
Published on Web 06/17/2003

Computational Study of the Halogen Atom−Benzene Complexes

Meng-Lin Tsao, Christopher M. Hadad,* and Matthew S. Platz*

Contribution from the Department of Chemistry, The Ohio State University, 100 West 18th Avenue, Columbus, Ohio 43210

Received March 11, 2003; E-mail: hadad.1@osu.edu; platz.1@osu.edu

Abstract: The structures of halogen atom−benzene complexes were investigated by modern DFT and ab initio computational methods. The spectroscopic properties of the complexes are also predicted and are in good agreement with experiment where such data have been reported. The fluorine atom−benzene complex is predicted to be a σ complex due to the strength of a C−F bond. The chlorine atom−benzene complex is predicted to have an η_1 π complex structure, which is only slightly more favorable (1.1 kcal/mol with the BH&HLYP/6-311++G** method including the ZPE correction) than a σ complex but is significantly more stable (4.4 kcal/mol with the BH&HLYP/6-311++G** method including the ZPE correction) than the η_6 π complex. The bromine and iodine benzene complexes are also predicted to prefer an η_1 π complex structure.

Introduction

In 1955 Russell and Brown studied the reaction of chlorine atoms with 2,3-dimethylbutane (DMB).[1] They discovered that the selectivity of chlorine atoms for tertiary relative to primary C−H bonds of DMB increased dramatically in the presence of benzene and other aromatic hydrocarbons.

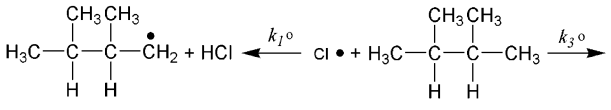

DMB

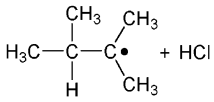

In a series of papers, Russell postulated that chlorine atom and benzene form a hexahapto (η_6) π-type complex usually written with chlorine residing over the center of symmetry of the benzene ring (**2a**).[2]

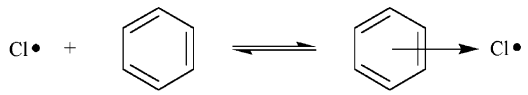

2a

To account for the variation of the selectivity (k_{3o}/k_{1o}) with benzene concentration, Russell proposed that the π complex **2a**, which is less reactive and more selective than a free chlorine atom in its reactions with DMB, is in equilibrium with benzene and chlorine atom.

Subsequently, Skell and co-workers studied the k_{3o}/k_{1o} ratio over a much broader range of DMB concentrations and discovered conditions where the complex was not in equilibrium with its components.[3] Specifically, the observed selectivity approached that of a free chlorine atom at high DMB concentrations, while the selectivity was high and nearly invariant with [DMB] at very low DMB concentrations. The Skell group presented arguments in favor of a σ complex (or chlorocyclohexadienyl radical) structure σ-**2c** as the high-selectivity intermediate.[3,4]

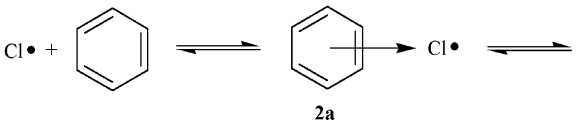

2a

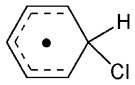

σ-2c

The chlorine atom−benzene complex has been generated by pulse radiolysis and has a strong and broad absorption at 490 nm.[5] This absorption resembles spectra observed with many aromatic charge-transfer complexes and seemingly supports the π complex structure.[2b]

Sergeev et al. reported the EPR spectra of the chlorine atom−benzene complex in the solid phase at 77 K and suggested that this complex has a structure intermediate between that of a pure hexahapto π complex and a pure chlorocyclohexadienyl radical (e.g., π-**2c**).[6]

(1) Russell, G. A.; Brown, H. C. *J. Am. Chem. Soc.* **1955**, *77*, 4031.
(2) (a) Russell, G. A. *J. Am. Chem. Soc.* **1957**, *79*, 2977. (b) Russell, G. A. *J. Am. Chem. Soc.* **1958**, *80*, 4987. (c) Russell, G. A. *J. Am. Chem. Soc.* **1958**, *80*, 4997.
(3) Skell, P. S.; Baxter, H. N., III; Taylor, C. K. *J. Am. Chem. Soc.* **1983**, *105*, 120.
(4) Skell, P. S.; Baxter, H. N., III; Tanko, J. M.; Chebolu, V. *J. Am. Chem. Soc.* **1986**, *108*, 6300.
(5) (a) Bühler, R. E.; Ebert, M. *Nature (London)* **1967**, *214*, 1220. (b) Bühler, R. E. *Helv. Chim. Acta* **1968**, *51*, 1558.

10.1021/ja035095u CCC: $25.00

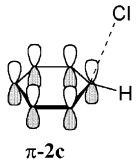

π-2c

Ingold, Scaiano, and co-workers generated free chlorine atom and the chlorine atom−benzene complex by laser flash photolysis methodology.[7,8] This group was able to obtain absolute rate constants for reactions of both free and complexed chlorine atom and determined that the equilibrium constant for complexation was $K_{Cl} = 200\ M^{-1}$ at ambient temperature. The Ottawa group came out strongly in favor of a π complex structure.

Walling has posited that the π complex is the spectroscopically observed species and the species that abstracts hydrogen from 2,3-dimethylbutane, but could be in equilibrium with the σ complex.[9] Benson has argued in favor of the σ complex as the species that absorbs strongly at 490 nm, which is in rapid cage equilibrium with an unobserved π complex.[10]

In a cogent review, Tanko has pointed out that the data require the presence of only free chlorine atom and one type of complex.[11]

Russell's classic work beautifully illustrates the reactivity−selectivity principle and many additional concepts in physical organic chemistry. The controversy over the structure of the chlorine atom−benzene complex motivated us to study this system as well as other halogen atom−benzene complexes by modern computational methods.

Computational Methodology

Scheme 1 shows three models of the halogen atom−benzene complexes studied in this section. The first model is a hexahapto (η_6) complex with the halogen atom sitting over the center of symmetry of the benzene ring (C_{6v} symmetry), the second model is a dihapto (η_2) complex with the halogen atom sitting over the center of a carbon−carbon bond of the benzene ring (C_s symmetry), and the third model is a monohapto (η_1) complex with the halogen atom sitting over a single carbon atom of the benzene ring (C_s symmetry).

Geometries of these model structures were fully optimized using density functional theory (DFT)[12] with Becke's three-parameter hybrid functional using the LYP correlation functional (B3LYP)[13] and with the half-and-half functional (BH&HLYP).[14] The molecular symmetry of the model structures was maintained during the optimizations. Two different basis sets were used in the DFT calculations. For hydrogen, carbon, fluorine, and chlorine atoms, the standard 6-31G* (6D) basis set[15] was used as the small basis set (SB), and the extended

Scheme 1

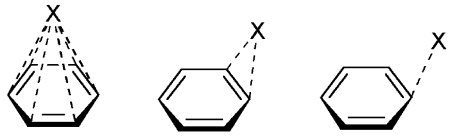

	η_6	η_2	η_1
X = F	**1a**	**1b**	**1c**
= Cl	**2a**	**2b**	**2c**
= Br	**3a**	**3b**	**3c**
= I	**4a**	**4b**	**4c**

6-311++G** (5D) basis set[16,17b] was used as the big basis set (BB). For bromine atom, the 6-311G(2d) (6D) basis set[17] was used as SB and the 6-311+G(2d) (5D) basis set[17] was used as BB. For iodine atom, the effective core potentials (ECPs) from Stuttgart and Dresden (SDD)[18] were used as both SB and BB. The calculated $\langle S^2 \rangle$ values were found to be 0.75−0.76 for the η_6 and η_2 structures and 0.75−0.86 for the η_1 structures. These $\langle S^2 \rangle$ values improved to 0.75−0.76 after the projection/annihilation process.

Vibrational frequency calculations were performed for the B3LYP/SB and BH&HLYP/SB optimized geometries to analyze the nature of the complexes (minimum or transition state) and were used to account for zero-point vibrational energy (ZPE) differences, enthalpies, and Gibbs free energies. The ZPE corrections were unscaled.

The potential energy surface of the monohapto halogen−benzene complexes (**1c**−**4c**) as a function of the shortest carbon−halogen bond distances (r_{C-X}) was calculated using the partial geometry optimizations of the complexes with a given set of frozen r_{C-X} values. These calculations were performed using the B3LYP/SB and BH&HLYP/SB methods. Single-point energies at the CASPT2(7,7) level of theory[19] were also calculated for the BH&HLYP/SB partially optimized geometries. The basis sets used in the CASPT2 calculations, denoted as SB′, were 6-31G* (5D) for H, C, F, and Cl, 6-311G(2d) (5D) for Br, and the ECPs of Cowan-Griffin-relativistic core ab initio model potentials (CG-AIMP)[20] with the contraction of (3s4p3d) for iodine. The (7,7) active space of the CASPT2 calculations consisted of six π MOs of the aromatic ring plus one p AO of the halogen atom which was perpendicular to the plane of the aromatic ring.

Reaction field calculations were performed in the presence of benzene as a solvent using the polarizable continuum model (PCM) of Tomasi and co-workers.[21] For these PCM calculations, single-point energies of halogen−benzene complexes in benzene were computed using the B3LYP and BH&HLYP methods with the SB and BB basis sets for their optimized geometries at the same computational level in the gas phase.

For comparison purposes, single-point energies of the BH&HLYP/SB optimized geometries of the complexes were calculated using various theoretical methods, such as fourth-order Møller−Plesset theory including single, double, and quadruple excitations (MP4(SDQ)),[22] complete active space self-consistent field (CASSCF)[23] and its second-

(6) Sergeev, G. B.; Pukhovskii, A. V.; Smirnov, V. V. *Russ. J. Phys. Chem.* **1983**, *57*, 589.
(7) Bunce, N. J.; Ingold, K. U.; Landers, J. P.; Lusztyk, J.; Scaiano, J. C. *J. Am. Chem. Soc.* **1985**, *107*, 5464.
(8) (a) Ingold, K. U.; Lusztyk, J.; Raner, K. D. *Acc. Chem. Res.* **1990**, *23*, 219. (b) Rander, K. D.; Lusztyk, J.; Ingold, K. U. *J. Phys. Chem.* **1989**, *93*, 564. (c) Rander, K. D.; Lusztyk, J.; Ingold, K. U. *J. Am. Chem. Soc.* **1989**, *110*, 3519.
(9) Walling, C. *J. Org. Chem.* **1988**, *53*, 305.
(10) Benson, S. W. *J. Am. Chem. Soc.* **1993**, *115*, 6969.
(11) Tanko, J. M.; Suleman, N. K. In *Energetics of Organic Free Radicals*; Simões, J. A. S., Greenberg, A., Liebman, J. F., Eds.; Chapman & Hall: New York, 1996; Chapter 8.
(12) (a) Parr, R. G.; Yang, W. *Density-Functional Theory of Atoms and Molecules*; Oxford University Press: Oxford, 1989. (b) Labanowski, J. W.; Andzelm, J. *Density Functional Methods in Chemistry*; Springer: New York, 1991.
(13) (a) Becke, A. D. *J. Chem. Phys.* **1993**, *98*, 5648. (b) Lee, C.; Yang, W.; Parr, R. G. *Phys. Rev. B* **1988**, *37*, 785. (c) Miehlich, B.; Savin, A.; Stoll, H.; Preuss, H. *Chem. Phys. Lett.* **1989**, *157*, 200.
(14) Becke, A. D. *J. Chem. Phys.* **1993**, *98*, 1372.
(15) Hariharan, P. C.; Pople, J. A. *Theor. Chim. Acta* **1973**, *28*, 213.
(16) Krishnan, R.; Binkley, J. S.; Seeger, R.; Pople, J. A. *J. Chem. Phys.* **1980**, *72*, 650.
(17) (a) Frisch, M. J.; Pople, J. A.; Binkley, J. S. *J. Chem. Phys.* **1984**, *80*, 3265. (b) Clark, T.; Chandrasekhar, J.; Schleyer, P. v. R. *J. Comput. Chem.* **1983**, *4*, 294.
(18) (a) Schwerdtfeger, P.; Dolg, M.; Schwarz, W. H. E.; Bowmaker. G. A.; Boyd, P. D. W. *J. Chem. Phys.* **1989**, *91*, 1762. (b) Bergner, A.; Dolg, M.; Kuechle, W.; Stoll, H.; Preuss, H. *Mol. Phys.* **1993**, *80*, 1431.
(19) (a) Anderson, K.; Malmqvist, P.-Å.; Roos, B. O.; Sadlej, A. J.; Wolinski, K. *J. Phys. Chem.* **1990**, *94*, 5483. (b) Anderson, K.; Malmqvist, P.-Å.; Roos, B. O. *J. Chem. Phys.* **1992**, *96*, 1218. (c) Anderson, K.; Roos, B. O. *Int. J. Quantum Chem.* **1993**, *45*, 591.
(20) Barandiaran, Z.; Seijo, L. *J. Chem. Phys.* **1994**, *101*, 4049.
(21) (a) Miertus, S.; Tomasi, J. *Chem. Phys.* **1982**, *65*, 239. (b) Miertus, S.; Scrocco, E.; Tomasi, J. *Chem. Phys.* **1981**, *55*, 117. (c) Tomasi, J.; Persico, M. *Chem. Rev.* **1994**, *94*, 2027. (d) Cossi, M.; Barone, V.; Cammi, R.; Tomasi, J. *Chem. Phys. Lett.* **1996**, *255*, 327. (e) Cramer, C. J.; Truhlar, D. G. *Chem. Rev.* **1999**, *99*, 2161.

order perturbation theory correction (CASPT2),[19] coupled cluster with single and double substitutions and perturbative inclusion of triple excitations (CCSD(T)),[24] and coupled cluster with double substitutions and perturbative inclusion of triple excitations using Brueckner orbitals (BD(T)).[25] Multilevel energy computations were performed using the complete basis set (CBS) methods of Petersson and co-workers (CBS-QB3)[26] for fluorine atom−benzene complexes. A similar method, denoted as CBS-QBH&H, was applied to the calculations of chlorine atom−benzene complexes by modifying the first step of the CBS-QB3 procedure by replacing the B3LYP geometry optimization with an optimization at the BH&HLYP level, and including the scaled ZPE difference between the B3LYP and BH&HLYP methods in the second step of the multilevel calculations. The ZPE corrections were scaled by 0.99 for these two methods.[26b] However, significant spin contaminations were found in the Hartree−Fock wave functions during the post-HF calculations of some of the η_1 structures. This spin contamination problem will be discussed in the next section.

UV−vis absorption spectra of the B3LYP/BB and BH&HLYP/BB optimized geometries of the halogen−benzene complexes were estimated using the time-dependent density functional theory (TD-DFT)[27] method. Excitation energies of chlorine atom−benzene complexes (**2**) were also calculated using the CASSCF(7,7)/SB′ and CASPT2(7,7)/SB′ methods with the BH&HLYP/SB optimized geometries. Atomic charges and spin densities were computed using the natural population analysis (NPA)[28] phase of the natural bond orbital (NBO)[29] analysis.

DFT and single-reference post-HF calculations were carried out with the Gaussian 98 suite of programs.[30] The multireference calculations (CASSCF and CASPT2) were performed using the MOLCAS 5.0 suite of programs.[31]

Results and Discussion

Fluorine Atom−Benzene Complex. The η_6, η_2, and η_1 complexation models of Scheme 1 were investigated for the benzene−F complex using B3LYP and BH&HLYP methods with the standard 6-31G* (SB) and extended 6-311++G** (BB) basis sets. These DFT geometry optimizations led to one stationary structure for each of the individual complexation models. Because more than one stationary point was found on the potential energy surface (PES) of the η_1 benzene−Cl complex (Figure 3), the PES of the η_1 benzene−F complex was explored to confirm the number of stationary points of this η_1 complex (Figure S1, Supporting Information). Only one stationary point was found as a minimum on the PES of the η_1 benzene−F complex along the coordinate of the carbon−fluorine bond distance. The DFT optimized geometries of η_6

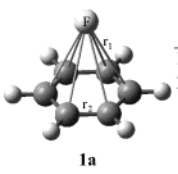

Methods	r_1	r_2
BH&HLYP/SB	3.220	1.387
BH&HLYP/BB	3.460	1.385
B3LYP/SB	3.083	1.397
B3LYP/BB	3.232	1.396

1a

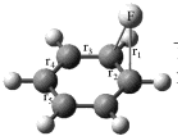

Methods	r_1	r_2	r_3	r_4	r_5
BH&HLYP/SB	2.285	1.396	1.393	1.378	1.397
BH&HLYP/BB	2.234	1.399	1.394	1.373	1.401
B3LYP/SB	2.134	1.419	1.405	1.386	1.412
B3LYP/BB	2.181	1.418	1.403	1.382	1.413

1b

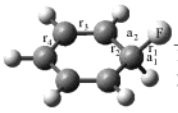

Methods	r_1	r_2	r_3	r_4	a_1	a_2
BH&HLYP/SB	1.398	1.490	1.357	1.412	104.5	109.4
BH&HLYP/BB	1.408	1.487	1.354	1.411	103.8	109.0
B3LYP/SB	1.423	1.496	1.367	1.419	104.0	109.4
B3LYP/BB	1.445	1.491	1.364	1.416	102.9	108.7

1c

Figure 1. Optimized geometries of the benzene−F complexes **1a**−**c**. Bond distances (r) and bond angles (a) are shown in Å and deg, respectively.

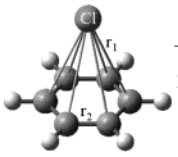

Methods	r_1	r_2
BH&HLYP/SB	3.739	1.387
BH&HLYP/BB	3.809	1.386
B3LYP/SB	3.687	1.397
B3LYP/BB	3.768	1.395

2a

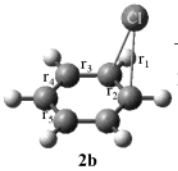

Methods	r_1	r_2	r_3	r_4	r_5
BH&HLYP/SB	2.793	1.399	1.393	1.379	1.397
BH&HLYP/BB	2.806	1.397	1.391	1.377	1.395
B3LYP/SB	2.774	1.415	1.402	1.389	1.409
B3LYP/BB	2.776	1.412	1.400	1.386	1.407

2b

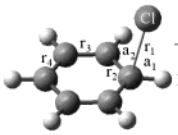

Methods	r_1	r_2	r_3	r_4	a_1	a_2
BH&HLYP/SB	2.583	1.403	1.380	1.391	83.2	96.9
BH&HLYP/BB	2.595	1.400	1.378	1.389	82.9	96.9
B3LYP/SB	2.580	1.415	1.388	1.402	82.7	97.6
B3LYP/BB	2.583	1.412	1.385	1.400	82.7	97.5

π-2c

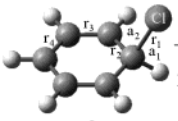

Methods	r_1	r_2	r_3	r_4	a_1	a_2
BH&HLYP/SB	1.921	1.471	1.361	1.408	98.9	107.7
BH&HLYP/BB	1.918	1.470	1.358	1.406	98.8	107.6
B3LYP/SB	---	---	---	---	---	---
B3LYP/BB	---	---	---	---	---	---

σ-2c

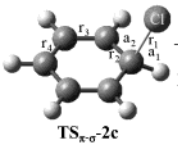

Methods	r1	r2	r3	r4	a_1	a_2
BH&HLYP/SB	2.088	1.445	1.367	1.402	93.4	104.7
BH&HLYP/BB	2.082	1.443	1.364	1.400	93.2	104.6
B3LYP/SB	---	---	---	---	---	---
B3LYP/BB	---	---	---	---	---	---

$TS_{π-σ}$-2c

Figure 2. Optimized geometries of the benzene−Cl complexes **2a**−**c**. Bond distances (r) and bond angles (a) are shown in Å and deg, respectively.

(22) (a) Krishnan, R.; Pople, J. A. *Int. J. Quantum Chem.* **1978**, *14*, 91. (b) Trucks, G. W.; Salter, E. A.; Sosa, C.; Bartlett, R. J. *Chem. Phys. Lett.* **1988**, *147*, 359. (c) Trucks, G. W.; Watts, J. D.; Salter, E. A.; Bartlett, R. J. *Chem. Phys. Lett.* **1988**, *153*, 490.

(23) (a) Roos, B. O. In *Ab Initio Methods in Quantum Chemistry*; Lawley, K. P., Ed.; Wiley: New York, 1987; Vol. 2, p 399. (b) Roos, B. O. *Adv. Chem. Phys.* **1987**, *69*, 339. (c) Roos, B. O. *Int. J. Quantum Chem. Symp.* **1980**, *14*, 175.

(24) (a) Purvis, G. D.; Bartlett, R. J. *J. Chem. Phys.* **1982**, *76*, 1910. (b) Scuseria, G. E.; Janssen, C. L.; Schaefer, H. F., III. *J. Chem. Phys.* **1988**, *89*, 7382. (c) Scuseria, G. E.; Schaefer, H. F., III. *J. Chem. Phys.* **1989**, *90*, 3700. (d) Pople, J. A.; Head-Gordon, M.; Raghavachari, K. *J. Chem. Phys.* **1987**, *87*, 5968.

(25) (a) Handy, N. C.; Pople, J. A.; Head-Gordon, M.; Raghavachari, K.; Trucks, G. W. *Chem. Phys. Lett.* **1989**, *164*, 185. (b) Dykstra, C. E. *Chem. Phys. Lett.* **1977**, *45*, 466.

(26) (a) Ochterski, J. W.; Petersson, G. A.; Montgomery, J. A., Jr. *J. Chem. Phys.* **1996**, *104*, 2598. (b) Montgomery, J. A., Jr.; Frisch, M. J.; Ochterski, J. W.; Petersson, G. A. *J. Chem. Phys.* **1999**, *110*, 2822.

(27) Casida, M. E.; Jamorski, C.; Casida, K. C.; Salahub, D. R. *J. Chem. Phys.* **1998**, *108*, 4439.

(28) Reed, A. E.; Weinstock, R. B.; Weinhold, F. *J. Chem. Phys.* **1985**, *83*, 735.

(29) Reed, A. E.; Curtiss, L. A.; Weinhold, F. *Chem. Rev.* **1988**, *88*, 899.

(30) Frisch, M. J.; Trucks, G. W.; Schlegel, H. B.; Scuseria, G. E.; Robb, M. A.; Cheeseman, J. R.; Zakrzewski, V. G.; Montgomery, J. A., Jr.; Stratmann, R. E.; Burant, J. C.; Dapprich, S.; Millam, J. M.; Daniels, A. D.; Kudin, K. N.; Strain, M. C.; Farkas, O.; Tomasi, J.; Barone, V.; Cossi, M.; Cammi, R.; Mennucci, B.; Pomelli, C.; Adamo, C.; Clifford, S.; Ochterski, J.; Petersson, G. A.; Ayala, P. Y.; Cui, Q.; Morokuma, K.; Malick, D. K.; Rabuck, A. D.; Raghavachari, K.; Foresman, J. B.; Cioslowski, J.; Ortiz, J. V.; Baboul, A. G.; Stefanov, B. B.; Liu, G.; Liashenko, A.; Piskorz, P.; Komaromi, I.; Gomperts, R.; Martin, R. L.; Fox, D. J.; Keith, T.; Al-Laham, M. A. Peng, C. Y.; Nanayakkara, A.; Gonzalez, C.; Challacombe, M.; Gill, P. M. W.; Johnson, B. G.; Chen, W.; Wong, M. W.; Andres, J. L.; Head-Gordon, M.; Replogle, E. S.; Pople, J. A. *Gaussian 98* (Revision A.9); Gaussian, Inc.: Pittsburgh, PA, 1998.

(31) Andersson, K.; Barysz, M.; Bernhardsson, A.; Blomberg, M. R. A.; Cooper, D. L.; Fleig, T. Fülscher, M. P.; de Graaf, C. Hess, B. A.; Karlström, G.; Lindh, R.; Malmqvist, P.-Å.; Neogrády, P.; Olsen, J.; Roos, B. O.; Sadlej, A. J.; Schütz, M.; Schimmelpfennig, B.; Seijo, L.; Serrano-Andrés, L.; Siegbahn, P. E. M.; Stålring, J.; Thorsteinsson, T.; Veryazov, V.; Widmark, P.-O. *MOLCAS* Version 5; Lund University: Sweden, 2000.

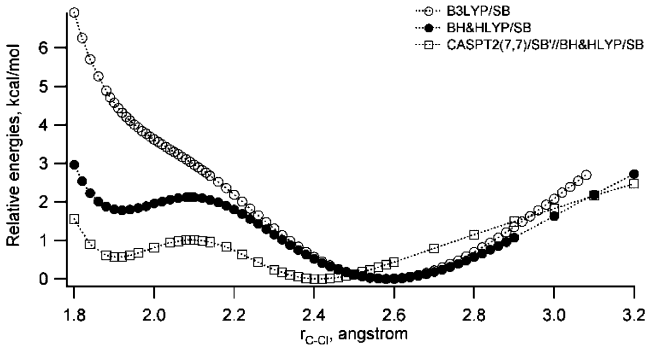

Figure 3. Calculated potential energy surface of the η_1 benzene−Cl complex (**2c**) as a function of the C−Cl bond distance using the theoretical levels of B3LYP/SB (open circles), BH&HLYP/SB (filled circles), and CASPT2(7,7)/SB′//BH&HLYP/SB (squares).

Table 1. Relative Energies (kcal/mol, bottom-of-well energies unless otherwise noted) and Entropies (eu) of the η_1 (**1c**), η_6 (**1a**), and η_2 (**1b**) Benzene−F Complexes, and Free Fluorine Atom with Benzene Using Various Computational Methods

computational method	**1c** (η_1)	**1a** (η_6)	**1b** (η_2)	Bz + F[c]
BH&HLYP/SB	0.00	29.75	25.27	31.03
BH&HLYP/BB	0.00	28.30	22.13	28.93
B3LYP/SB	0.00	34.79	20.46	36.54
B3LYP/BB	0.00	33.13	15.29	33.96
MP4(SDQ)/SB//BH&HLYP/SB	0.00[b]	24.41	24.81	25.43
CCSD(T)/SB//BH&HLYP/SB	0.00[b]	28.45	25.94	29.63
BD(T)/SB//BH&HLYP/SB	0.00[b]	29.11	26.60	30.28
CBS-QB3	0.00[b]	14.47	26.27	36.01
CASPT2/BB//BH&HLYP/SB	0.00	30.99	29.53	
PCM//BH&HLYP/SB	0.00	31.54	25.73	32.36
PCM//BH&HLYP/BB	0.00	31.37	22.20	30.72
PCM//B3LYP/SB	0.00	36.02	20.18	37.19
PCM//B3LYP/BB	0.00	34.68	14.67	34.97
H_{298}//BH&HLYP/SB[a]	0.00	28.83	24.97	31.04
G_{298}//BH&HLYP/SB[a]	0.00	30.22	24.71	24.34
S_{298}//BH&HLYP/SB	0.00	−4.68	0.85	22.48

[a] Thermal corrected energies. [b] Significant spin contamination was found in the Hartree−Fock wave function. [c] The sum of the energies of benzene and free fluorine atom.

(**1a**), η_2 (**1b**), and η_1 (**1c**) benzene−F complexes are given in Figure 1, and the calculated electronic and thermal energies of **1a**−**c** are summarized in Table 1.

Optimization within η_1 complexation gives the most stable structure **1c** for the benzene−F complex. Such favorable η_1 complex geometries have been determined for the isoelectronic complex of HO• radical with benzene and other aromatic hydrocarbons.[32] In **1c**, the shortest carbon−fluorine bond length (r_1) is calculated to be 1.40−1.41 Å for the BH&HLYP geometries and 1.42−1.45 Å for the B3LYP geometries, the F−C−C bond angle (a_2) is ∼109°, and the F−C−H bond angle (a_1) is 103−105° (Figure 1). Thus, the *ipso*-carbon in **1c** is sp^3 hybridized, and **1c** can be described as the 6-fluorocyclohexadienyl radical, a σ-type benzene−F complex. This is consistent with the reported matrix EPR[33] and IR[34] studies at 4 and 14 K, respectively.

The complexation enthalpy ($\Delta H_{complex}$) of the formation of σ complex **1c** can be deduced from the experimental heats of formation of **1c**, benzene, and fluorine atom. At 298 K,

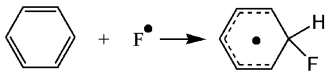

$$\Delta H_{complex} = H_f(C_6H_6F) - H_f(C_6H_6) - H_f(F)$$

$\Delta H_f(C_6H_6F) = 14.8$ kcal/mol,[35] $\Delta H_f(C_6H_6) = 19.8$ kcal/mol,[36] and $\Delta H_f(F) = 19.8$ kcal/mol.[36] Thus, the experimental value of $\Delta H_{complex}$ for the formation of **1c** is −24.8 kcal/mol at 298 K.

Inspection of the data in Table 1 reveals that the calculated stabilization energy of the σ complex formation of **1c** is 28.9−31.0 kcal/mol with the BH&HLYP methods including the ZPE correction (Supporting Information). The complexation energies derived from the B3LYP methods are about 5 kcal/mol higher, but those obtained from coupled-cluster theory (CCSD(T) and BD(T)) are very close to the BH&HLYP energies. With the inclusion of ZPE differences at the BH&HLYP/SB levels, the CCSD(T) and BD(T) methods predicted the stabilization energy to be 29.0 and 29.7 kcal/mol, respectively. Note that the T_1 diagnostic of Lee and Taylor[37] for the CCSD(T) calculation of **1c** was found to be ∼0.03. This measure refers to the multireference character of **1c**.[37,38] Due to the multireference character, the energies of **1c** derived from the single-reference correlated method of MP4(SDQ) and multilevel method of CBS-QB3, which uses the MP4(SDQ) method in its fourth step, are questionable. However, the inclusion of triple excitations in the CCSD(T) and BD(T) calculations seems to be effective in correcting for a single-reference treatment of a weakly multireference problem.[38]

Solvation effects were examined computationally using the PCM method with benzene as solvent. Compared to the gas-phase energies at the same computational level, the solvation effect of benzene stabilizes **1c** by 1−2 kcal/mol relative to the energetic sum of the free fluorine atom and benzene molecule.

The change of entropy during the complexation of fluorine atom and benzene to form **1c** was calculated with the BH&HLYP/SB method. It was found to be 22.5 eu (Table 1). Therefore, the entropy term disfavors the formation of the benzene−F complex **1c** by 6.7 kcal/mol at 298 K.

For the η_6 benzene−F complex (**1a**), the BH&HLYP calculations show that **1a**, possessing C_{6v} symmetry, has two degenerate (e_1) vibrational imaginary frequencies. As to the B3LYP calculations, even though no imaginary vibrational frequency was found for the optimized geometry of **1a** with this method, its B3LYP wave function was found to have internal instability; that is, it is more like an electronic excited state. When a stable B3LYP wave function was obtained, the geometry optimization failed to converge using this wave function. Nonetheless, the DFT calculations demonstrate that **1a** is not a stable structure to represent the benzene−F complex. Energetically, **1a** was found to be at least 28 kcal/mol less stable than the σ complex **1c** at various reliable computational levels (Table 1).

(32) (a) Davis, D. D.; Bollinger, W.; Fischer, S. *J. Phys. Chem.* **1975**, *79*, 293. (b) Barckholtz, C.; Barckholtz, T. A.; Hadad, C. M. *J. Phys. Chem. A* **2001**, *105*, 140, and references therein. (c) Tokmakov, I. V.; Lin, M. C. *J. Phys. Chem. A* **2002**, *106*, 11309.
(33) Cochran, E. L.; Adrian, F. J.; Bowers, Y. A. *J. Phys. Chem.* **1970**, *74*, 2083.
(34) Jacox, M. E. *J. Phys. Chem.* **1982**, *86*, 670.
(35) Grover, J. R.; Wen, Y.; Lee, Y. T.; Shobatake, K. *J. Chem. Phys.* **1988**, *89*, 938.
(36) Tsang, W. In *Energetics of Organic Free Radicals*; Simões, J. A. S., Greenberg, A., Liebman, J. F., Eds.; Chapman & Hall: New York, 1996; Chapter 2.
(37) Lee, T. J.; Taylor, P. R. *Int. J. Quantum Chem., Quantum Chem. Symp.* **1989**, *23*, 199.
(38) Cramer, C. J. *Essentials of Computational Chemistry−Theories and Models*; Wiley: New York, 2002.

Table 2. Calculated Spin Density and Atomic Charge of Halogen Atom in the Halogen Atom−Benzene Complexes Using the Natural Population Analysis (NPA) Method

	BH&HLYP/SB		B3LYP/SB	
complex	spin density	atomic charge	spin density	atomic charge
σ-**1c** (η_1-Bz/F)	0.041	−0.409	0.048	−0.388
1a (η_6-Bz/F)	0.995	−0.003	0.973	−0.024
1b (η_2-Bz/F)	0.790	−0.181	0.608	−0.304
π-**2c** (η_1-Bz/Cl)	0.741[a]	−0.221	0.673	−0.272
σ-**2c** (η_1-Bz/Cl)	0.193	−0.165	*b*	*b*
TS$_{\pi-\sigma}$-**2c** (η_1-Bz/Cl)	0.373	−0.251	*b*	*b*
2a (η_6-Bz/Cl)	0.994	−0.006	0.983	−0.018
2b (η_2-Bz/Cl)	0.788	−0.191	0.706	−0.260
π-**3c** (η_1-Bz/Br)	0.807	−0.169	0.728	−0.234
3a (η_6-Bz/Br)	0.996	−0.005	0.984	−0.018
3b (η_2-Bz/Br)	0.830	−0.154	0.747	−0.226
π-**4c** (η_1-Bz/I)	0.892	−0.097	0.814	−0.166
4a (η_6-Bz/I)	0.996	−0.006	0.994	−0.009
4b (η_2-Bz/I)	0.898	−0.093	0.821	−0.162

[a] There are 18% and 15% net α-spin on the *para* and *ortho* carbons, respectively, and 1% and 11% net β-spin on the *ipso* and *meta* carbons, respectively. [b] Not a stationary point with the B3LYP/SB computational method.

Regarding the η_2 benzene−F complex (**1b**), both BH&HLYP and B3LYP calculations show that **1b** is a transition state in nature because of the observation of one imaginary vibrational frequency. By following the normal vibrational mode (a″) of this imaginary frequency, it led to the σ complex (**1c**). Therefore, **1b** is acting as the transition state for the fluorine atom in **1c** to "travel" around the benzene ring, and the energy difference between **1b** and **1c** corresponds to the barrier for this process. The data in Table 1 suggest that this barrier height is more than 20 kcal/mol at most of the computational levels.

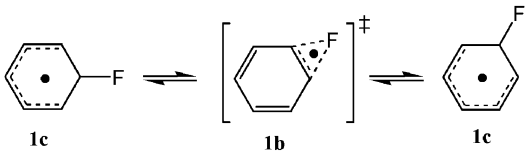

The computed spin density and atomic charge of fluorine atom in structures **1a**−**c** are listed in Table 2. For the σ complex **1c**, only 4−5% of spin density was found remaining on the fluorine atom, and a significant negative charge (about −0.4) was obtained on F, due to the large electronegativity of F. As to the η_6 complex **1a**, the α-spin on the fluorine atom was almost untransferred, and zero partial charge was obtained on F. This indicates an extremely weak interaction between the F atom and benzene molecule. The η_2 complex **1b** shows medium spin density and atomic charge properties between **1c** and **1a**.

As shown in Table 3, TD-DFT calculations at the B3LYP/BB level predict that σ complex **1c** should absorb very weakly in the visible region at around 470 nm and strongly in the UV region at around 309 nm. These absorptions resemble those of the cyclohexadienyl radical ($C_6H_7^{\bullet}$) with a small red-shift on the visible band and a slight blue-shift on the UV absorption band relative to $C_6H_7^{\bullet}$. The predicted UV−vis absorptions of this σ-type complex are in excellent agreement with the experimental spectrum of cyclohexadienyl radical ($C_6H_7^{\bullet}$) produced by the LFP method.[7,39]

Table 3. Calculated UV−Vis Absorption Maxima (λ_{max}) and Oscillator Strengths (*f*) for the Halogen Atom−Benzene Complexes Using the TD-DFT Method

	BH&HLYP/BB		B3LYP/BB	
complex	λ_{max}, nm	*f*	λ_{max}, nm	*f*
σ-**1c** (η_1-Bz/F)	402	0.004	470	0.004
	279	0.078	309	0.069
1a (η_6-Bz/F)	*a*	*a*	*b*	*b*
1b (η_2-Bz/F)	476	0.007	400	0.112
	428	0.185		
π-**2c** (η_1-Bz/Cl)	456	0.208	458	0.177
	335	0.050	306	0.029
σ-**2c** (η_1-Bz/Cl)	416	0.003	*c*	*c*
	296	0.016		
2a (η_6-Bz/Cl)	*a*	*a*	*b*	*b*
2b (η_2-Bz/Cl)	481	0.213	484	0.184
π-**3c** (η_1-Bz/Br)	482	0.179	493	0.178
	352	0.031	313	0.022
3a (η_6-Bz/Br)	*a*	*a*	*b*	*b*
3b (η_2-Bz/Br)	489	0.183	513	0.176
π-**4c** (η_1-Bz/I)	491	0.138	556	0.170
	367	0.013	318	0.009
4a (η_6-Bz/I)	*a*	*a*	317	0.026
4b (η_2-Bz/I)	488	0.139	564	0.164
$C_6H_7^{\bullet}$	394	0.001	453	0.001
	287	0.091	316	0.089

[a] No strong absorption was found above 300 nm. [b] Internal instability was found for the B3LYP wave functions. [c] Not a stationary point with the B3LYP/BB method.

Although TD-DFT calculations predict that the η_2 benzene−F complex (**1b**) would absorb very intensely in the visible region, this visible absorption is not expected to be observable since **1b** is a transition state and is high in energy content relative to **1c**.

Chlorine Atom−Benzene Complex. Among the η_6, η_2, and η_1 complexation models of Scheme 1, the BH&HLYP calculations of the benzene−Cl complex led to five stationary structures and the B3LYP calculation of the benzene−Cl complex found only three stationary structures. The DFT optimized geometries of these stationary structures of the benzene−Cl complex are shown in Figure 2, and their calculated electronic and thermal energies with various computational methods are summarized in Table 4.

One stationary point was found for the BH&HLYP calculations of the η_6 benzene−Cl complex **2a**, originally postulated by Russell[2] and used frequently as the representative structure of the π-type benzene−Cl complex.[2−4,6−10] As shown in Figure 2, the optimized geometry of **2a** demonstrates a long C−Cl bond distance (3.7−3.8 Å) and negligible change of the C−C bond length in benzene (1.39 Å). These geometrical parameters illustrate a very weak interaction between Cl and benzene in **2a**. Furthermore, the BH&HLYP calculations show that **2a**, possessing C_{6v} symmetry, has two degenerate (e_1) imaginary vibrational frequencies (Supporting Information). This suggests that **2a** is actually not a stable structure to represent the benzene−Cl complex. Similar results were reported for the calculated structure of the η_6 benzene−Cl_2 complex (C_{6v}) with the RHF and MP2 methods.[40]

As in the calculations of η_6 benzene−F complex **1a**, the B3LYP methods could not treat **2a** properly. Even though a B3LYP optimized geometry of **2a** could be obtained, and without any imaginary vibrational frequencies, the B3LYP wave

(39) Berho, F.; Rayez, M.-T.; Lesclaux, R. *J. Phys. Chem. A* **1999**, *103*, 5501.

(40) Matsuzawa, H.; Osamura, Y. *Bull. Chem. Soc. Jpn.* **1997**, *70*, 1531.

Table 4. Relative Energies (kcal/mol, bottom-of-well energies unless otherwise noted) and Entropies (eu) of the π-Type η_1 (π-**2c**), σ-Type η_1 (σ-**2c**), Transition State η_1 (**TS**$_{\pi-\sigma}$-**2c**), η_6 (**2a**), and η_2 (**2b**) Benzene−Cl Complexes, and Free Chlorine Atom with Benzene Using Various Computational Methods

method	π-**2c** (η_1)	σ-**2c**	**2a** (η_6)	**2b** (η_2)	**TS**$_{\pi-\sigma}$-**2c**	Bz + Cl[h]
BH&HLYP/SB[a]	0.00	1.78	5.13	0.51	2.12	6.28
BH&HLYP/BB[b]	0.00	1.75	4.59	0.52	2.15	5.53
B3LYP/SB	0.00	*f*	9.58	0.48	*f*	10.68
B3LYP/BB	0.00	*f*	9.08	0.55	*f*	9.82
MP4(SDQ)/SB[a]	0.00[e]	−3.04[e]	−8.12	−9.07	−0.47[e]	−6.75
CCSD(T)/SB[a]	0.00[e]	−0.33[e]	0.42	−1.41	1.01[e]	1.94
BD(T)/SB[a]	0.00[e]	0.29[e]	1.87	0.04	1.37[e]	3.40
CBS-QBH&H	0.00[e]	−3.73[e]	−13.64	*g*	*g*	7.31
CASPT2/SB′[c]	0.00	0.57	3.54[a]	1.06[a]	1.01	*g*
PCM//BH&HLYP/SB	0.00	1.25	6.99	0.86	1.32	7.00
PCM//BH&HLYP/BB	0.00	1.05	6.48	0.81	1.20	6.18
PCM//B3LYP/SB	0.00	*f*	12.10	0.82	*f*	11.19
PCM//B3LYP/BB	0.00	*f*	11.67	0.78	*f*	10.30
H_{298}[a,d]	0.00	0.89	4.01	0.04	0.81	6.05
G_{298}[a,d]	0.00	2.00	6.77	1.29	2.36	0.92
S_{298}[a]	0.00	−3.73	−9.24	−4.18	−5.19	17.21

[a] Using BH&HLYP/SB optimized geometries. [b] Using BH&HLYP/BB optimized geometries. [c] Using BH&HLYP/SB partially optimized geometries (see Figure 3). [d] Thermal corrected energies. [e] Significant spin contamination was found in the Hartree−Fock wave function. [f] Not a stationary point with the B3LYP method. [g] Not determined. [h] The sum of the energies of benzene and free chlorine atom.

function of this structure was found to be unstable. When a stable B3LYP wave function was generated, the geometry optimization failed to converge using this wave function.

The BH&HLYP calculations of the η_1 benzene−Cl complex (**2c**) possessing C_s symmetry gave three stationary points: two minima and one transition state (Figure 3). The same number of stationary points was observed on the PES of **2c** using the CASPT2(7,7)/SB′//BH&HLYP/SB method, but only one stationary point was obtained using B3LYP methods (Figure 3).

One minimum (π-**2c**) that is observable by all three methods (BH&HLYP, CASPT2, and B3LYP) indicates a long carbon−chlorine bond distance. The calculated C−Cl bond distance is ∼2.6 Å with the DFT methods and ∼2.4 Å with the CASPT2 method (Figures 2 and 3). The spin density calculations of this intermediate predict that ∼70% of the spin remains on the chlorine atom and ∼30% is transferred to the aromatic ring system (Table 2). These results have the character of a π-type complex (π-**2c**).

Another local minimum, which was observed by the BH&HLYP and CASPT2 methods, but not the B3LYP method, demonstrates a σ carbon−chlorine bond distance. The C−Cl bond length in this intermediate is ∼1.9 Å with the BH&HLYP and CASPT2 methods, and the calculated Cl−C−C bond angle (a_2) is 108° (Figures 2 and 3). This illustrates that the *ipso*-carbon in this intermediate is sp^3 hybridized. Furthermore, the spin density distribution in this intermediate predicts that ∼20% of the spin density remains on the chlorine atom and ∼80% is transferred to the aromatic ring system (Table 2). Thus, this intermediate is a σ-type complex (σ-**2c**).

The third stationary point observed by the BH&HLYP and CASPT2 methods was a transition state (**TS**$_{\pi-\sigma}$-**2c**) connecting π-**2c** and σ-**2c**. The calculated carbon−chlorine bond distance in **TS**$_{\pi-\sigma}$-**2c** (∼2.1 Å) was between those of π-**2c** and σ-**2c** (Figures 2 and 3).

Regarding the η_2 benzene−Cl complex (**2b**), both BH&HLYP and B3LYP calculations found one stationary point within this model. The calculated C−Cl bond distance in **2b** is about 2.8 Å, which is only 0.2 Å longer than that in π-**2c** (Figure 2). The spin density of Cl in **2b** is found to be only ∼4% higher than that in π-**2c** (Table 2). These results demonstrate the similarity between **2b** and π-**2c**. However, the DFT calculations reveal that **2b** has an imaginary vibrational frequency and is a transition state. Following the vibrational mode (a″) of this imaginary frequency led to the π-type η_1 complex (π-**2c**). Therefore, **2b** is the transition state for the chlorine atom in π-**2c** to "travel" around the benzene ring, and the energy difference between **2b** and π-**2c** corresponds to the barrier to this process.

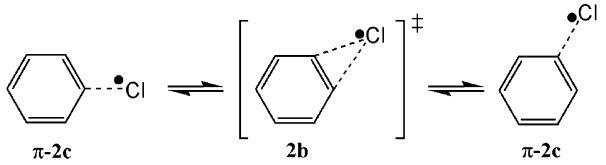

Inspection of the relative energies of the five different benzene−Cl complex structures in Table 4 reveals that π-**2c**, the π-type η_1 complex, is the most stable structure with the BH&HLYP method. Using the BH&HLYP method with ZPE correction (Supporting Information), the η_6 complex (**2a**) is 4−5 kcal/mol less stable than π-**2c**, the σ-type η_1 complex (σ-**2c**) is ∼1 kcal/mol less stable than π-**2c**, the barrier height for π-**2c** to convert to σ-**2c** is 1.3−1.4 kcal/mol, and the activation energy for the Cl atom in π-**2c** to "travel" around the aromatic ring is ∼0.5 kcal/mol. Furthermore, the complexation energy for the formation of π-**2c** is predicted to be ∼5.2 kcal/mol exothermic using the BH&HLYP/BB+ZPE method.

The B3LYP method failed to locate the σ-type η_1 complex (σ-**2c**). In addition, this method has a tendency to overstabilize π-type η_1 (π-**2c**) and η_2 (**2b**) by ∼4.3 kcal/mol compared to the BH&HLYP energies. As a result, the relative energies of the η_6 complex (**2a**) and free chlorine atom with benzene are ∼4.3 kcal/mol higher in energy.

The single-reference MP4(SDQ), CBS-QBH&H, and CCSD(T) calculations disagree with the DFT prediction of π-**2c** as the most stable benzene−Cl complex structure, while the BD(T) method still favors the most stable π-**2c**. This discrepancy is due to the fact that the η_1 complex (σ- and π-**2c**) contains multireference character, which can significantly affect the interpretation of the single-determinant correlated calculations.

The single-reference MP4(SDQ) and CCSD methods are very sensitive to the multireference character of the HF reference wave functions. During the calculations of **2c** using these methods, the $\langle S^2 \rangle$ values of 1.20−1.26 were obtained in the HF reference wave functions compared to $\langle S^2 \rangle = 0.75$ for a pure radical. The severe spin contamination refers to the multireference character of **2c**. Indeed, the T_1 diagnostic of Lee and Taylor,[37] one measure of the multireference character in the CCSD(T) calculations of **2c**, yielded T_1 values in the range 0.03−0.04. Note that a value above 0.02 has been suggested as warranting some caution in the interpretation of single-reference CCSD results.[38] Therefore, the multireference character of **2c** makes the MP4(SDQ), CBS-QBH&H, and CCSD(T) results doubtful. The multireference character can also be problematic quantitatively for the BD(T) method even though π-**2c** was computed as the most stable structure with this method.

For the DFT (BH&HLYP and B3LYP) calculations of **2c**, spin contamination was found to be moderate. The $\langle S^2 \rangle$ values

obtained are in the range 0.78−0.86 and are improved to 0.75−0.76 after the projection/annihilation process.

The multireference CASPT2 calculations predict that π-**2c** is the most stable benzene−Cl complex structure. The η_6 complex (**2a**) is predicted to be 3.5 kcal/mol higher in energy than π-**2c**. Over a barrier height of ∼1 kcal/mol, π-**2c** can be converted to the σ-type η_1 complex (σ-**2c**), which is ∼0.6 kcal/mol less stable than π-**2c**. Furthermore, the activation energy for the Cl atom in π-**2c** to "travel" around the aromatic ring is ∼1.1 kcal/mol. These results are in remarkable agreement with the BH&HLYP calculations.

Solvation effects, computed using the PCM model, with DFT methods and benzene as a solvent show slight changes on the relative energies of complex structures of interest (Table 4). These energy changes are within 1 kcal/mol except that the relative energies of the η_6 complex increase by ∼2 kcal/mol. In general, the presence of a dielectric field corresponding to benzene solvent tends to stabilize the η_1 and η_2 complexes but destabilizes the η_6 complex compared to free Cl and benzene.

The entropy term of π-**2c** was computed to be ∼17.2 cal/mol·K more positive than the separated Cl and benzene molecule (Table 4). This means that the entropy term should reduce the free energy for the formation of π-**2c** by ∼5.1 kcal/mol at 298 K. Therefore, the complexation enthalpy is calculated to be exothermic by 6.1 kcal/mol, but the Gibbs free energy of the complexation process decreases to ∼1 kcal/mol exoergic with the BH&HLYP/SB method. In addition, the entropy term is unfavorable for all other complexation structures by 1−3 kcal/mol at 298 K as compared to π-**2c**.

As shown in Table 3, TD-DFT calculations predict that the η_1 π-type complex (π-**2c**) will absorb very strongly in the visible region at around 460 nm and less strongly in the UV region at around 306 nm. This is in excellent agreement with the reported absorption maximum of the CT band of the benzene−Cl complex at 490 nm.[5,7] No strong absorption was found above 300 nm for the TD-DFT calculations of the η_6 complex.

For the TD-DFT calculations of the η_1 σ-type complex (σ-**2c**), a weak absorption in the visible region and a stronger one in the UV region were predicted, similar to those predicted results for the cyclohexadienyl radical (Table 3).

Although TD-DFT predicts that the η_2 benzene−Cl complex (**2b**) would absorb very intensely in the visible region with absorption maximum at ∼480 nm, this visible absorption is unlikely to be responsible for the experimentally observed CT band since **2b** is predicted to be a transition state.

To confirm the TD-DFT results, the vertical excitation energies of these benzene−Cl complex structures were computed using the multireference CASSCF and CASPT2 methods (Table 5). The CASPT2 calculations predict that π-**2c** will absorb intensely at 469 and 319 nm, σ-**2c** will absorb intensely only at 311 nm, **2b** (η_2) could absorb strongly at 448 nm, and **2a** (η_6) will not have a strong absorption above 300 nm. The CASPT2-predicted UV−vis absorptions are in excellent agreement with the TD-DFT results. Thus, both energetically and spectroscopically, the η_1 π-type complex (π-**2c**) is the best structure to represent the benzene−Cl complex and is responsible for the species with high selectivity in the chlorination reaction of 2,3-dimethylbutane in the presence of aromatic solvent.

Table 5. Vertical Excitation Energies of the Chlorine Atom−Benzene Complexes

complex	state	CASSCF,[a] eV	CASPT2,[a] eV	CASPT2,[a] nm	w^b	osc. strength (f)[c]
π-**2c** (η_1)	$1^2A'$				0.78	
	$1^2A''$	3.06	2.47	502	0.76	0.002
	$2^2A'$	3.08	2.64	469	0.77	0.085
	$3^2A'$	4.75	3.89	319	0.74	0.133
	$4^2A'$	5.20	4.46	278	0.73	0.087
	$2^2A''$	5.43	4.59	270	0.76	0.003
σ-**2c** (η_1)	$1^2A'$				0.79	
	$1^2A''$	2.73	2.44	509	0.79	0.000
	$2^2A'$	5.23	3.53	352	0.77	0.001
	$3^2A'$	4.79	3.58	346	0.76	0.001
	$2^2A''$	6.38	3.99	311	0.76	0.127
	$4^2A'$	6.84	4.66	266	0.74	0.210
2b (η_2)	$1^2A'$				0.78	
	$1^2A''$	3.08	2.46	504	0.76	0.002
	$2^2A'$	3.56	2.77	448	0.76	0.146
	$2^2A''$	4.25	3.84	323	0.77	0.001
	$3^2A'$	5.04	4.46	278	0.76	0.013
2a (η_6)	1^2A_1				0.79	
	1^2B_2	3.48	2.85	435	0.77	0.000
	1^2B_1	3.48	2.85	434	0.77	0.000
	2^2B_2	4.25	3.98	312	0.78	0.000
	3^2B_2	5.42	4.63	268	0.76	0.000
	2^2B_1	5.41	4.64	267	0.77	0.000
	3^2B_1	5.37	4.83	257	0.77	0.000
	2^2A_1	6.37	5.62	221	0.76	0.024
	1^2A_2	7.61	7.15	173	0.77	0.000

[a] Using the BH&HLYP/6-31G* geometries with the (7,7) active space and the 6-31G* (5D) basis set. [b] The weight of the CASSCF wave function. [c] Oscillator strength.

Bromine Atom−Benzene Complex. The calculations of the benzene−Br complex are similar to those of the benzene−Cl complex except that the η_1 σ complex does not exist for the BH&HLYP and B3LYP calculations of the benzene−Br complex. Only one stationary point could be obtained for the PES of the η_1 benzene−Br complex (**3c**) as a function of the C−Br bond distance (Figure S2, Supporting Information).

The DFT optimized geometries of η_6 (**3a**), η_2 (**3b**), and the above-mentioned η_1 (**3c**) benzene−Br complex are given in Figure 4, and the calculated electronic and thermal energies of **3a**−**c** are summarized in Table 6.

The BH&HLYP optimized geometry of the η_6 complex (**3a**) displays a long C−Br bond distance (4.1−4.3 Å) and negligible change of the C−C bond length in benzene (1.39 Å). These geometrical parameters illustrate a very weak interaction between Br and benzene in **3a**. Like the η_6 benzene−Cl complex (**2a**), the BH&HLYP calculations show that **3a**, possessing C_{6v} symmetry, has two degenerate (e_1) imaginary vibrational frequencies (Supporting Information).

As in the B3LYP calculations of the η_6 benzene−F and η_6 benzene−Cl complexes, the B3LYP methods could not treat **3a** properly. The B3LYP optimization of the ground-state structure of **3a** failed and the wave function shows internal instability, although no imaginary vibrational frequencies were found.

The DFT optimized geometry of the η_1 benzene−Br complex (**3c**) most resembles that of the η_1 π-type benzene−Cl complex (π-**2c**). The calculated C−Br bond distance in **3c** is 2.8−2.9 Å (Figure 4), and the spin density of the Br atom in **3c** was calculated to be ∼80% with ∼20% spin density being transferred to the aromatic ring (Table 2). Therefore, like π-**2c**, **3c** is a π-type complex.

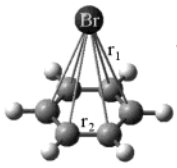

Methods	r_1	r_2
BH&HLYP/SB	4.070	1.387
BH&HLYP/BB	4.288	1.385
B3LYP/SB	3.817	1.398
B3LYP/BB	3.996	1.395

3a

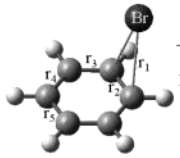

Methods	r_1	r_2	r_3	r_4	r_5
BH&HLYP/SB	2.981	1.398	1.392	1.380	1.394
BH&HLYP/BB	3.021	1.394	1.390	1.379	1.392
B3LYP/SB	2.952	1.413	1.402	1.390	1.407
B3LYP/BB	2.968	1.409	1.399	1.388	1.404

3b

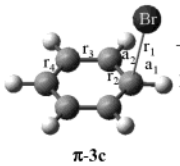

Methods	r_1	r_2	r_3	r_4	a_1	a_2
BH&HLYP/SB	2.818	1.399	1.382	1.389	82.7	96.0
BH&HLYP/BB	2.861	1.395	1.381	1.387	82.2	95.9
B3LYP/SB	2.790	1.412	1.389	1.401	81.6	97.2
B3LYP/BB	2.802	1.408	1.387	1.398	81.3	97.1

π-3c

Figure 4. Optimized geometries of the benzene−Br complexes **3a**−**c**. Bond distances (*r*) and bond angles (*a*) are shown in Å and deg, respectively.

Table 6. Relative Energies (kcal/mol, bottom-of-well energies unless otherwise noted) and Entropies (eu) of the η_1 (**3c**), η_6 (**3a**), and η_2 (**3b**) Benzene−Br Complexes, and Free Bromine Atom with Benzene Using Various Computational Methods

computational method	**3c** (η_1)	**3a** (η_6)	**3b** (η_2)	Bz + Br[c]
BH&HLYP/SB	0.00	3.79	0.22	5.35
BH&HLYP/BB	0.00	2.84	0.17	3.82
B3LYP/SB	0.00	7.16	0.25	8.74
B3LYP/BB	0.00	6.08	0.23	6.79
MP4(SDQ)/SB//BH&HLYP/SB	0.00[b]	−7.28	−8.98	−4.93
CCSD(T)/SB//BH&HLYP/SB	0.00[b]	1.47	−1.31	4.03
BD(T)/SB//BH&HLYP/SB	0.00[b]	2.88	0.07	5.44
CASPT2/BB//BH&HLYP/SB	0.00	2.98	0.25	
PCM//BH&HLYP/SB	0.00	6.10	0.41	5.50
PCM//BH&HLYP/BB	0.00	6.04	0.36	3.78
PCM//B3LYP/SB	0.00	9.17	0.47	8.80
PCM//B3LYP/BB	0.00	7.89	0.48	6.65
H_{298}//BH&HLYP/SB[a]	0.00	2.63	−0.30	5.06
G_{298}//BH&HLYP/SB[a]	0.00	5.42	1.23	0.33
S_{298}//BH&HLYP/SB	0.00	−9.35	−5.12	15.87

[a] Thermal corrected energies. [b] Significant spin contamination was found in the Hartree−Fock wave function. [c] The sum of the energies of benzene and free bromine atom.

The DFT geometry of the η_2 benzene−Br complex (**3b**) is similar to that of the η_2 benzene−Cl complex (**2b**). The calculated C−Br bond distance in **3b** is about 3.0 Å, which is only 0.16 Å longer than that in **3c** (Figure 4). Like **2b**, the η_2 benzene−Br complex **3b** is a transition state (one imaginary vibrational frequency) for the bromine atom in **3c** to "travel" around the benzene ring.

Inspection of the relative energies in Table 6 reveals that **3c**, the π-type η_1 complex, is the most stable structure using the DFT, BD(T), and CASPT2 methods. With these computational methods, the η_6 complex (**3a**) is ∼3 kcal/mol higher and the η_2 complex (**3b**) is 0.1−0.3 kcal/mol higher than **3c** in energy content, and the complexation energy for the formation of **3c** is predicted to be exothermic by ∼4−5 kcal/mol.

For the MP4(SDQ) and CCSD(T) calculations of **3c**, a $\langle S^2 \rangle$ value of 1.23 was observed in the HF reference wave functions. The severe spin contamination refers to the multireference character of **3c**. Additionally, the T_1 diagnostic of Lee and Taylor[37] in the CCSD(T) calculations of **3c** was found to be 0.034. This confirms the multireference character of **3c** and makes the MP4(SDQ) and CCSD(T) results questionable.

The solvation effects (PCM with benzene as solvent) on the relative energies of the benzene−Br complex are very small for **3c** and **3b** but are significant for the η_6 complex (**3a**). With benzene as solvent, **3a** is destabilized by 2−3 kcal/mol with the DFT methods.

The absolute entropy of **3c** was computed to be ∼16 cal/mol·K more positive than the separated Br atom and benzene molecule (Table 6). This means that the entropy term should disfavor the formation of the most stable complex (**3c**) by ∼4.7 kcal/mol at 298 K. Furthermore, the entropy term disfavors **3a** and **3b** by 2.8 and 1.5 kcal/mol, respectively, relative to **3c** at 298 K.

TD-DFT calculations predict that the η_1 π-type benzene−Br complex (**3c**) will absorb very strongly in the visible region with an absorption maximum around 482−493 nm (Table 3). This is in good agreement with the reported experimental data.[41−43] The CT absorption of the benzene−Br complex has been reported to have an absorption maximum at 510−560 nm in the condensed phase[41,42] and at 469 nm in an argon matrix at 17 K.[43]

The TD-DFT calculations of the η_6 complex (**3a**) predict that this species lacks a strong absorption above 300 nm. As for the η_2 benzene−Br complex (**3b**), it was predicted to have a strong absorption in the visible region. However, **3b** is a transition state. Thus, it is reasonable to assign the CT benzene−Br complex to structure **3c**, the η_1 π-type complex.

Iodine Atom−Benzene Complex. The calculations of the benzene−I complex present a now familiar pattern. Three different structures were obtained using the DFT calculations. They are η_6 (**4a**), η_2 (**4b**), and π-type η_1 (**4c**) benzene−I complexes. Only one stationary point was present on the PES of the η_1 benzene−I complex (**4c**) along the coordinate of the C−I bond distance (Figure S3, Supporting Information). Note that this PES was found to be very flat in the region near the minimum.

The DFT optimized geometries of η_6 (**4a**), η_2 (**4b**), and η_1 (**4c**) benzene−I complexes are given in Figure 5, and the calculated electronic and thermal energies of **4a**−**c** are summarized in Table 7.

Inspection of the BH&HLYP optimized geometries of the benzene−I complex in Figure 5 reveals that the C−I bond distance is estimated to be 2.82−2.86 Å in the η_1 complex (**4c**), 2.98−3.02 Å in the η_2 complex (**4b**), and 4.07−4.29 Å in the η_6 complex (**4c**). The difference in C−I bond distance is only 0.16 Å between **4b** (η_2) and **4c** (η_1) and is about 1.2−1.3 Å between **4a** (η_6) and **4c** (η_1). The lengthy C−I bond distances illustrate a weak interaction between the iodine atom and benzene in these π-type complex structures.

The vibrational frequency calculations with DFT (BH&HLYP and B3LYP) methods show that **4a**, possessing C_{6v} symmetry, has two degenerate (e_1) imaginary frequencies and that **4b**, possessing C_s symmetry, has one imaginary frequency (Supporting Information). Hence, both **4a** and **4b** are not stable

(41) Barra, M.; Smith, K. *J. Org. Chem.* **2000**, *65*, 1892.
(42) Bühler, R. E. *J. Phys. Chem.* **1972**, *76*, 3220.
(43) Engdahl, A.; Nelander, B. *J. Chem. Phys.* **1982**, *77*, 1649.

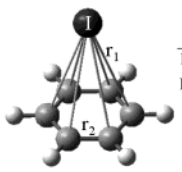

Methods	r_1	r_2
BH&HLYP/SB	4.197	1.387
BH&HLYP/BB	4.223	1.385
B3LYP/SB	4.312	1.397
B3LYP/BB	4.309	1.395

4a

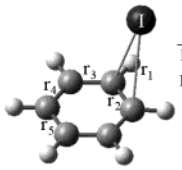

Methods	r_1	r_2	r_3	r_4	r_5
BH&HLYP/SB	3.315	1.394	1.390	1.383	1.391
BH&HLYP/BB	3.381	1.390	1.388	1.382	1.388
B3LYP/SB	3.264	1.409	1.400	1.392	1.404
B3LYP/BB	3.299	1.404	1.398	1.390	1.400

4b

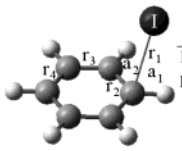

Methods	r_1	r_2	r_3	r_4	a_1	a_2
BH&HLYP/SB	3.194	1.394	1.384	1.388	81.4	95.6
BH&HLYP/BB	3.273	1.390	1.383	1.386	80.7	95.7
B3LYP/SB	3.136	1.407	1.392	1.399	80.7	96.7
B3LYP/BB	3.173	1.403	1.390	1.397	79.7	96.8

4c

Figure 5. Optimized geometries of the benzene−I complexes **4a**−**c**. Bond distances (*r*) and bond angles (*a*) are shown in Å and deg, respectively.

Table 7. Relative Energies (kcal/mol, bottom-of-well energies unless otherwise noted) and Entropies (eu) of the η_1 (**4c**), η_6 (**4a**), and η_2 (**4b**) Benzene−I Complexes, and Free Iodine Atom with Benzene Using Various Computational Methods

computational method	**4c** (η_1)	**4a** (η_6)	**4b** (η_2)	Bz + I[c]
BH&HLYP/SB	0.00	1.76	0.06	3.07
BH&HLYP/BB	0.00	1.30	0.07	2.13
B3LYP/SB	0.00	3.93	0.11	5.03
B3LYP/BB	0.00	3.01	0.13	3.53
MP4(SDQ)/SB//BH&HLYP/SB	0.00	−1.33	−0.79	0.00
CCSD(T)/SB//BH&HLYP/SB	0.00	−0.48	−0.09	0.92
BD(T)/SB//BH&HLYP/SB	0.00	1.44	−0.03	0.98
CASPT2/BB[a]//BH&HLYP/SB	0.00	1.76	0.00	
PCM//BH&HLYP/SB	0.00	3.47	0.13	2.38
PCM//BH&HLYP/BB	0.00	4.36	0.11	1.29
PCM//B3LYP/SB	0.00	5.73	0.23	4.19
PCM//B3LYP/BB	0.00	5.63	0.23	2.49
H_{298}//BH&HLYP/SB[b]	0.00	0.57	−0.51	2.74
G_{298}//BH&HLYP/SB[b]	0.00	4.06	1.31	−1.38
S_{298}//BH&HLYP/SB	0.00	−11.72	−6.10	13.80

[a] The 6-311++G** basis set for C, H and CG-AIMP with the contraction of (3s4p3d) for I were used. [b] Thermal corrected energies. [c] The sum of the energies of benzene and free iodine atom.

structures. Only the η_1 complex (**4c**) possessing C_s symmetry was predicted to be a minimum (no imaginary vibrational frequencies) on the PES of the benzene−I complex. These results are similar to the computational findings of the benzene−I_2 complex using DFT and ab initio calculations.[44]

Energetically, the η_6 complex (**4a**) is predicted to be 1.1, 1.3, and 1.6 kcal/mol less stable than the η_1 complex (**4c**) at the theoretical levels of BH&HLYP/BB, BD(T)/SB, and CASPT2/BB′, respectively, with the ZPE correction (Supporting Information) derived from the BH&HLYP/SB method. The complexation energy for the formation of **4c** is estimated to be exothermic by 1.9 and 0.7 kcal/mol using the BH&HLYP/BB and BD(T)/SB methods, respectively, with the BH&HLYP/SB ZPE correction.

As shown in Table 3, the TD-DFT calculations of **4c** using the BH&HLYP/BB method predict a strong visible absorption band of **4c** at 491 nm. This is in excellent agreement with the experimental observation of the CT band of the benzene−I complex at 465−500 nm produced from flash photolysis methods[42] and at 470 and 475 nm in an argon matrix at 17 K.[45]

However, the MP4(SDQ) and CCSD(T) methods predict that the η_6 complex (**4a**) is 1.3 and 0.5 kcal/mol, respectively, more stable than **4c** even though no considerable spin contamination was found in the HF reference wave functions ($\langle S^2 \rangle = 0.78$) and the T_1 diagnostic value[37] in the CCSD(T) calculation of **4c** was found to be smaller than 0.02. Since the TD-DFT calculations of **4a** showed no strong UV−vis absorption above 300 nm, **4a** could not be the benzene−I complex to give the CT absorption band. Thus, the MP4(SDQ) and CCSD(T) results are very questionable, and for reasons that are not obvious.

The η_2 benzene−I complex (**4b**) was predicted to be within 0.1 kcal/mol relative to **4c** except for the problematic MP4(SDQ) method (Table 7). Since the vibrational mode of its imaginary frequency demonstrates that **4b** is a transition state for the iodine atom to "walk" around the benzene ring, the small energy difference between **4b** and **4c** suggests that the iodine atom in **4c** moves from the top of one carbon atom of benzene to the top of another carbon atom of benzene very easily. Thus, the iodine atom is "delocalized" in **4c**.

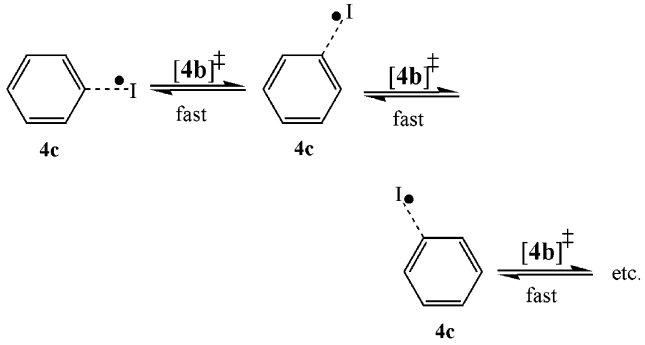

The absolute entropy of **4c** was computed to be ∼14 cal/mol·K more positive than the separated iodine atom and benzene molecule (Table 7); therefore, the entropy term disfavors the formation of **4c** by ∼4.1 kcal/mol at 298 K. Furthermore, the entropy term disfavors **4a** and **4b** by 3.5 and 1.8 kcal/mol, respectively, relative to **4c** at 298 K.

Conclusions

The structures of the chlorine atom−benzene complex and other halogen atom−benzene complexes were investigated using DFT and ab initio calculations. The η_6 benzene−Cl complex **2a**, frequently written as the π-type benzene−Cl complex, was found to have two degenerate imaginary vibrational frequencies and was estimated to have no strong absorptions above 300 nm. The η_1 σ-type complex (6-chlorocyclohexadienyl radical, σ-**2c**) was found to not be the global minimum on the potential energy surface of the benzene−Cl complex. Theory predicts that σ-**2c** has a strong absorption in the UV region but an extremely weak absorption in the visible region, similar to the cyclohexadienyl radical. The most stable structure of the benzene−Cl complex was predicted to be an η_1 π-type complex (π-**2c**), in which the

(44) (a) Mebel, A. M.; Lin, H. L.; Lin, S. H. *Int. J. Quantum Chem.* **1999**, *72*, 307. (b) Grozema, F. C.; Zijlstra, R. W. J.; Swart, M.; Duijnen, P. T. V. *Int. J. Quantum Chem.* **1999**, *75*, 709.

(45) Engdahl, A.; Nelander, B. *J. Chem. Phys.* **1983**, *78*, 6563.

chlorine atom resides over a carbon atom of a benzene molecule with a C−Cl bond distance of 2.58−2.60 Å. The estimated UV−vis absorption maxima of π-**2c** are at 469 and 319 nm, and with strong oscillator strengths using the CASPT2 method. This complex (π-**2c**) is computed to be 5.2 kcal/mol more stable than an isolated benzene molecule and chlorine atom with the BH&HLYP/BB+ZPE method. In π-**2c**, the spin density is calculated to have ∼74% population on chlorine atom and ∼26% on the rest of the components of the complex with the natural population analysis (NPA) method. There are 18% and 15% net α-spin on the *para* and *ortho* carbons, respectively, and 1% and 11% net β-spin on the *ipso* and *meta* carbons, respectively. The prediction of π-**2c** as the most stable structure of the benzene−Cl complex is consistent with reported observations of UV−vis,[5,7] ESR,[6] kinetics,[7,8,11] and product studies.[1−4]

6-Fluorocyclohexadienyl radical (**1c**), an η_1 σ-type complex, was computed to be the minimum energy geometry for the benzene−F complex. This complex (**1c**) is predicted to have a UV−vis spectrum (λ_{max} = 309 nm) similar to that of cyclohexadienyl radical and is computed to be 28−30 kcal/mol lower in enthalpy than an isolated benzene molecule and fluorine atom at 298 K. The NPA spin density of fluorine atom in **1c** is estimated to be 4−5%.

For the benzene−Br and benzene−I complexes, the computed most stable geometry for each (**3c** and **4c**) resembles π-**2c** of the benzene−Cl complex. Complexes **3c** and **4c** were predicted to have strong absorptions in the visible region (λ_{max} = 482 and 491 nm, respectively, using the TD-BH&HLYP method) and with absorption maxima similar to the observed CT bands of the benzene−Br and benzene−I complexes in the literature.[41−43,45] These complexes were computed to be 4−5 and <2 kcal/mol, respectively, more stable than an isolated benzene molecule and halogen atom (Br or I). The NPA spin density of halogen atom (Br or I) in **3c** and **4c** is estimated to be 81% and 89%, respectively. The potential energy surface of the benzene−I complex is very flat. Thus, even though **4c** has C_s symmetry, the iodine atom in **4c** can "walk" over each carbon atom of the benzene molecule with a minimal barrier (<0.1 kcal/mol) so that **4c** can act like a molecule with a C_{6v} point group, especially at high temperatures.

Acknowledgment. Support of this work by the National Science Foundation is gratefully acknowledged. The authors are indebted to the Ohio Supercomputer Center for computational support. One of us (M.-L.T.) gratefully acknowledges a Presidential Fellowship of The Ohio State University.

Supporting Information Available: The calculated potential energy surface of the η_1 benzene−F, benzene−Br, and benzene−I complexes. Computational data including Cartesian coordinates of all optimized geometries, tables of electronic and thermal energies, vibrational frequencies, and TD-DFT absorption maxima and oscillator strengths. This material is available free of charge via the Internet at http://pubs.acs.org.

JA035095U